International Journal of Nephrology and Renovascular Disease

Dovepress

open access to scientific and medical research

Open Access Full Text Article

ORIGINAL RESEARCH

FGF23 modulates the effects of erythropoietin on gene expression in renal epithelial cells

This article was published in the following Dove Press journal:
International Journal of Nephrology and Renovascular Disease

Mitsuru Yashiro[1]
Masaki Ohya[1]
Toru Mima[1]
Yumi Ueda[2]
Yuri Nakashima[1]
Kazuki Kawakami[1]
Yohei Ishizawa[2]
Shuto Yamamoto[1]
Sou Kobayashi[1]
Takurou Yano[1]
Yusuke Tanaka[1]
Kouji Okuda[1]
Tomohiro Sonou[1]
Tomohiro Shoshihara[1]
Yuko Iwashita[1]
Yu Iwashita[1]
Kouichi Tatsuta[1]
Ryo Matoba[2]
Shigeo Negi[1]
Takashi Shigematsu[1]

[1]Department of Nephrology, Wakayama Medical University, Wakayama, Japan; [2]DNA Chip Research Inc., Minato, Japan

Background: FGF23 plays an important role in calcium–phosphorus metabolism. Other roles of FGF23 have recently been reported, such as commitment to myocardium enlargement and immunological roles in the spleen. In this study, we aimed to identify the roles of FGF23 in the kidneys other than calcium–phosphorus metabolism.

Methods: DNA microarrays and bioinformatics tools were used to analyze gene expression in mIMCD3 mouse renal tubule cells following treatment with FGF23, erythropoietin and/or an inhibitor of ERK.

Results: Three protein-coding genes were upregulated and 12 were downregulated in response to FGF23. Following bioinformatics analysis of these genes, PPARγ and STAT3 were identified as candidate transcript factors for mediating their upregulation, and STAT1 as a candidate for mediating their downregulation. Because STAT1 and STAT3 also mediate erythropoietin signaling, we investigated whether FGF23 and erythropoietin might show interactive effects in these cells. Of the 15 genes regulated by FGF23, 11 were upregulated by erythropoietin; 10 of these were downregulated following cotreatment with FGF23. Inhibition of ERK, an intracellular mediator of FGF23, reversed the effects of FGF23. However, FGF23 did not influence STAT1 phosphorylation, suggesting that it impinges on erythropoietin signaling through other mechanisms.

Conclusion: Our results suggest cross talk between erythropoietin and FGF23 signaling in the regulation of renal epithelial cells.

Keywords: FGF23, STAT1, PPARγ, DNA microarray, bioinformatics analysis, nonprotein-coding gene

Introduction

FGF23 is produced by osteoblasts when they sense an increase in the serum concentration of phosphate.[1] FGF23 produced by the osteoblasts induces renal epithelial cells to promote phosphorus diuresis. Simultaneously, FGF23 suppresses the intake of phosphate in the intestinal tract by inhibiting production of the active form of vitamin D in renal epithelial cells.[2–4] Moreover, FGF23 plays an important role in the onset of chronic kidney disease–mineral and bone disorder.[5] Thus, FGF23 plays important roles in Ca–P metabolism. Recently, new physiological roles have been found for FGF23, such as the commitment of myocardium enlargement,[6] proliferation of chondrocytes,[7] infiltration of neutrophils[8] and impairment of B lymphopoiesis.[9] Furthermore, we have reported that FGF23 is expressed in the spleen, which plays important roles in the immune system, and the regulation of FGF23 expression in the spleen differs

Correspondence: Toru Mima
Department of Nephrology, Wakayama Medical University, 811-1, Kimiidera, Wakayama 641-8510, Japan
Tel/Fax +81 73 441 0639
Email mimat@wakayama-med.ac.jp

submit your manuscript | www.dovepress.com
Dovepress
http://dx.doi.org/10.2147/IJNRD.S158422

from that of the bone.[10] In the spleen, plasmacytoid dendritic cells produce FGF23 and mature B cells express the FGF23 coreceptor, Klotho, suggesting that FGF23 plays an immunological role.[11] These results suggest that, in renal epithelial cells, FGF23 might have biological roles in addition to Ca–P metabolism. However, such additional roles have not been identified before now. It has been thought that they would be difficult to determine using conventional methods.

In vitro experiments are required to analyze the roles of FGF23 other than Ca–P metabolism because the serum level of calcium and phosphate would be changed by FGF23 administration in vivo and would subsequently influence gene expression in other tissues, including renal tubule epithelial cells. The mouse renal tubule epithelial cell line, mIMCD3, is a representative cell line which is frequently used for experiments relating to renal tubule epithelial cells and has been reported to express Klotho.[12] We confirmed the expression of both Klotho and FGF receptor 1 in mIMCD3 cells (Figure S1), demonstrating that this cell line is suitable for investigating the effects of FGF23. The expression of erythropoietin receptor in mIMCD3 cells was as same as that of erythroblast.

Recently, using exhaustive gene expression analyses with DNA microarrays followed by bioinformatics analysis, new pathogenetic mechanisms have been identified in diseases such as systemic lupus erythematosus[13] and systemic juvenile idiopathic arthritis.[14] New abnormalities and biological functions were clarified, which could not be achieved using conventional methods. To identify new biological roles of FGF23 in renal epithelial cells, we comprehensively analyzed gene expression in mIMCD3 cells following stimulation with FGF23. We used DNA microarrays and bioinformatics tools to identify candidate transcription factors for regulating differentially expressed genes.

Methods

Cell line and cell culture

mIMCD3 cells were purchased from Riken Cell Bank (Tsukuba, Japan) and cultured in Dulbecco's modified Eagle's medium/F12 medium supplemented with 10% fetal bovine serum (SH30079.03; Hyclone, Logan, UT, USA) at 37°C under 5% CO_2.

Extraction of RNA from mIMCD3 cells with or without FGF23 stimulation

mIMCD3 cells were stimulated with FGF23 for 4 h in order to identify not only those genes whose expression is induced by FGF23 but also those whose expression is suppressed through inhibitory mechanisms, such as microRNAs. The cells were cultured with or without 10 ng/mL FGF23 (2629FG; R&D Systems, Minneapolis, MN, USA)[15] for 4 h. Total RNA was then extracted using TRIzol reagents (Thermo Fisher Scientific, Waltham, MA, USA) according to the manufacturer's protocol. RNA was extracted from five replicate cultures in each treatment group. The concentration of extracted RNA was measured, and the quality was evaluated by electrophoresis.

Analysis of gene expression using DNA microarrays

To minimize variations in gene expression between replicate cultures, the RNA for microarray analysis was made by mixing 1 μg from each of the five replicates stimulated with FGF23. RNA from the five replicates not treated with FGF23 was mixed in the same way to make a control. The concentration and quality of these RNA preparations were determined using a Nanodrop ND-1000 spectrophotometer (Thermo Fisher Scientific) and an Agilent Bioanalyzer (Agilent Technologies, Santa Clara, CA, USA), as recommended by Agilent Technologies. Linear T7-based amplification was performed using 100 ng of each RNA preparation. Total RNA was amplified and labeled with Cy3 or Cy5 using an Agilent Low Input Quick Amp Labeling Kit, Two-color (Agilent Technologies), following the manufacturer's instructions. Yields of cRNA and the dye-incorporation rate were measured using a Nanodrop ND-1000 spectrophotometer and an Agilent Bioanalyzer. Hybridization was performed according to the Agilent 60-mer oligo microarray processing protocol, using the Agilent Gene Expression Hybridization Kit (Agilent Technologies). The labeled cRNA probes were hybridized overnight (17 h at 65°C) to Agilent Whole Mouse Genome oligo microarrays 8 × 60 K (Design ID: 028005). After washing, the microarrays were scanned using a G2505C Microarray Scanner (Agilent Technologies), and signal values were calculated using Agilent software. The median and SD of the background fluorescence level were calculated, and the probe for which the fluorescence intensity was less than the median background plus 2 × SD was considered to be not expressed. The Cy3/Cy5 ratios of all spots on the microarrays were normalized using the global ratio median normalization method. Changes in gene expression were quantified using the ratio of fluorescence values with FGF23 stimulation to those without FGF23 stimulation, obtained by calculating the geometric mean of the Cy3/Cy5 ratio from two microarray hybridization experiments. Upregulated genes were identified as those showing a with-FGF23-to-without-FGF23 ratio of more than 1.5, and for which both fluorescence values were

more than 30. This meant that the differences in fluorescence values with and without FGF23 were more than the background SD, 11. Downregulated genes were identified as those showing a with-FGF23-to-without-FGF23 ratio of less than 0.7, and again showing fluorescence values of more than 30 both with and without FGF23 stimulation.

Bioinformatics analysis

Bioinformatics analysis was conducted using oPOSSUM, version 3.0 (http://opossum.cisreg.ca/oPOSSUM3) to identify transcription factors that putatively regulate the differentially expressed genes.

Effects of FGF23 on gene expression induced by erythropoietin

mIMCD3 cells, on which the expression of EpoR was confirmed (Figure S1) and whose expression level of EpoR was as same as that of erythroblasts, were stimulated with 1 U/mL erythropoietin (959ME; R&D Systems),[16] with or without 10 ng/mL recombinant FGF23 protein, for 2 or 4 h at 37°C. After stimulation, cells were washed twice with medium. RNA was extracted using TRIzol reagents, as described above, and cDNA was synthesized from total RNA using a Transcriptor First-Strand cDNA synthesis Kit (Roche Diagnostics, Mannheim, Germany). qPCR assays for *Akt1s1* (Mm01203150_g1), *Ak4* (Mm00784745_g1), *Ankrd37* (Mm01344843_g1), *Bnip3* (Mm01275600_g1), *Cadps2* (Mm01137059_g1), *Krt17* (Mm00495207_g1), *Mgarp1* (Mm00471236_g1), *Mt1* (Mm00496660_g1), *Mt2* (Mm00809556_g1), *Pdk1* (Mm00554300_g1), *Pygl* (Mm01289790_g1), *Rgs16* (Mm00803317_g1), *Selenbp* (Mm01611432_g1), *Slc16a3* (Mm00446102_g1) and *Tmprss6* (Mm0055119_g1) were performed on an ABI 7500 System (Thermo Fisher Scientific) using TaqMan Gene Expression Assays (Thermo Fisher Scientific). *Gapdh* (Mm99999915_g1; Thermo Fisher Scientific) was used as a housekeeping gene to normalize expression values.

Western blot analysis of phosphorylated STAT1

mIMCD3 cells were stimulated with 5 U/mL erythropoietin,[17] with or without recombinant FGF23 protein at a concentration of 10, 20 or 50 ng/mL, for 15 min at 37°C. After stimulation, cells were washed twice with medium. After protein extraction using M-PER (Thermo Fisher Scientific) and a protein inhibitor, the protein concentration was determined using a Pierce BCA Protein Assay Kit (Thermo Fisher Scientific). A total of 10 µg protein and STAT1 control cell extracts (9173; Cell Signaling Technology, Danvers, MA, USA) were applied to each lane of polyacrylamide electrophoresis gels. After electrophoresis, proteins were transferred onto PVDF membranes using the Ezblot (AE-1460; ATTO Corp, Tokyo, Japan) reagent and a semi-dry blotting unit (WSE-4110 PoweredBLOT One; ATTO Corp) according to the manufacturer's instructions. Membranes were then blocked for 1 h at room temperature in a commercial blocking reagent (PVDF Blocking Reagent for Can Get Signal®; Toyobo, Osaka, Japan). After three washes with TBST, membranes were incubated with a rabbit anti-phospho-STAT1 antibody (7649S; Cell Signaling Japan, Tokyo, Japan) diluted in immunoreaction enhancer solution (1:1000, Can Get Signal Solution 1; Toyobo), overnight at 4°C. The membranes were washed three times with TBST and then incubated with horseradish peroxidase-conjugated donkey anti-rabbit IgG (ab16284; Abcam, Cambridge, UK) diluted in immunoreaction enhancer solution (1:5000, Can Get Signal Solution 2; Toyobo) for 1 h at room temperature. Membranes were then washed in TBST and processed following an enhanced chemiluminescence protocol (ECL Prime Western Blotting Detection Reagent; GE Healthcare, Little Chalfont, UK). Antibody binding was detected using a WSE-6100 LuminoGraph chemiluminescence imaging system (ATTO Corp), and was quantified using the CS Analyzer version 1.0.2 (ATTO Corp). Membranes were stripped using EzReprobe (ATTO Corp) and reprobed for GAPDH (1:1000, SC-25778; Santa Cruz Biotechnology, Dallas, TX, USA) as a protein loading control.

ERK mediation of the suppression of gene expression by FGF23

An ERK inhibitor, FR180204,[18] was purchased from Cayman Chemical (15544; Ann Arbor, MI, USA). mIMCD3 cells were stimulated with 1 U/mL erythropoietin and/or 10 ng/mL FGF23 with or without 1 µM FR180204, for 2 h. After stimulation, RNA was extracted and gene expression was analyzed using qPCR, as described above.

Statistical analysis

All values are expressed as the means ± SD, and statistical significance was determined using the Kruskal–Wallis analysis of variance followed by the post hoc Steel–Dwass test. All statistical computations were performed using JMP version 13.0 (SAS Institute Inc, Cary, NC, USA). $p < 0.05$ was considered statistically significant.

Results

Microarray analysis of gene expression induced by FGF23

DNA microarray analysis revealed that 26 genes were differentially expressed in mIMCD3 cells following FGF23 stimulation, compared with the same cells without FGF23 stimulation. The microarray data can be found on Gene Expression Omnibus (https://www.ncbi.nlm.nih.gov/geo/, GSE100847). Eight out of 26 genes were upregulated, and the remaining 18 were downregulated. Three out of eight upregulated genes were protein-coding genes (Table 1), and the remaining five were nonprotein coding (Table 2). Fifteen out of 18 downregulated genes were protein coding (Table 1), and the remaining three were nonprotein coding (Table 2). Three out of 15 downregulated protein-coding genes were identified as RIKEN genes, for which we could not perform expression analysis using qPCR.

Transcription factors putatively regulating differentially expressed genes

To identify mechanisms regulating gene expression, we performed a bioinformatics analysis to identify transcription factors with putative binding sites in the genes that were differentially expressed following FGF23 stimulation. Among the transcription factors with binding sites in FGF23-upregulated genes (Table 3), PPARγ and STAT3 were of greatest interest because they are known to be active in renal tubule epithelial cells. PPARγ mediates vitamin D activity in these cells.[19] STAT3 mediates the intracellular signaling of erythropoietin,[20] which is known to have effects on renal tubule epithelial cells, as well as protective effects on renal injury in patients with chronic kidney diseases.[21] The other transcription factors with binding sites in FGF23-upregulated genes are not known to act in renal tubule epithelial cells.

Among the transcription factors with binding sites in FGF23-downregulated genes (Table 4), STAT1 was of greatest interest because it is also known to mediate the intracellular signaling of erythropoietin.[20] The other transcription factors with binding sites in FGF23-downregulated genes are not known to act in renal tubule epithelial cells. These results suggest the possibility of cross talk between FGF23 and erythropoietin signaling in renal tubule epithelial cells.

FGF23 modulation of gene expression induced by erythropoietin in renal tubule epithelial cells

As determined by qPCR, the expression of *Rgs16* tended to be upregulated following FGF23 stimulation for 2 h but was not significantly upregulated by FGF23 stimulation for 4 h. The expression of *Krt17* and *Akt1s1* was upregulated by FGF23 stimulation as determined using microarry analysis but not using qPCR. These differences could be attributable to the methods used, with the microarray analysis making a direct comparison, whereas the qPCR made an indirect comparison using a reference gene. The direct comparison is more reliable, according to a previous report.[22] Expression of *Rgs16*, which tended to be upregulated in response to FGF23, was also upregulated following erythropoietin stimulation (Figure 1).

Table 1 Differentially expressed protein-coding genes following FGF23 stimulation

Gene symbol	Gene title	Accession no.	Fold change
Upregulated genes			
Rgs16	ref|Mus musculus regulator of G-protein signaling 16	NM_011267	1.514
Krt17	ref|Mus musculus keratin 17	NM_010663	1.509
Akt1s1	ref|Mus musculus AKT1 substrate 1 (proline-rich), transcript variant 3	NM_001290694	1.529
Downregulated genes			
Bnip3	ref|Mus musculus BCL2/adenovirus E1B-interacting protein 3	NM_009760	0.460
Ak4	ref|Mus musculus adenylate kinase 4, transcript variant 1	NM_001177602	0.666
Mt1	ref|Mus musculus metallothionein 1	NM_013602	0.565
Mt2	ref|Mus musculus metallothionein 2	NM_008630	0.575
Pdk1	ref|Mus musculus pyruvate dehydrogenase kinase, isoenzyme 1	NM_172665	0.619
Slc16a3	ref|Mus musculus solute carrier family 16 (monocarboxylic acid transporters), member 3	NM_030696	0.654
Cadps2	ref|Mus musculus Ca^{2+}-dependent activator protein for secretion 2, transcript variant 1	NM_153163	0.602
Tmprss6	ref|Mus musculus transmembrane serine protease 6	NM_027902	0.649
Selenbp1	ref|Mus musculus selenium-binding protein 1	NM_009150	0.621
Ankrd37	ref|Mus musculus ankyrin repeat domain 37	NM_001039562	0.624
2010300C02Rik	ref|Mus musculus RIKEN cDNA 2010300C02 gene	NM_028096	0.669
9530097N15Ri	gb|Mus musculus adult male urinary bladder cDNA, RIKEN full-length enriched library, clone: 9530097N15 product: unclassifiable, full insert sequence	AK020664	0.619
1700026L06Rik	ref|Mus musculus RIKEN cDNA 1700026L06 gene	NM_027283	0.648

Table 2 Differentially expressed noncoding genes following FGF23 stimulation

Gene symbol	Gene title	Affymetrix probe ID	Fold change
Upregulated genes			
chr11:58136882-58143829_R	lincRNA:chr11:58136882-58143829 reverse strand	10094	1.647
chr11:58136882-58143829_R	lincRNA:chr11:58136882-58143829 reverse strand	17372	1.950
chr1:59775022-59780348_F	lincRNA:chr1:59775022-59780348 forward strand	51425	1.561
chr9:95295459-95301266_F	lincRNA:chr9:95295459-95301266 forward strand	56437	1.514
chr11:58136882-58143829_R	lincRNA:chr11:58136882-58143829 reverse strand	61180	2.038
Downregulated genes			
chr4:56013597-56020622_R	lincRNA:chr4:56013597-56020622 reverse strand	44012	0.661
A_55_P2097048	Unknown	54292	0.468
chr6:112552041-112560067_R	lincRNA:chr6:112552041-112560067 reverse strand	59856	0.572

Table 3 Transcription factors putatively involved in the upregulation of genes following FGF23 stimulation

Transcription factor	JASPAR ID	No. of target gene hits	Hit genes	Biological function
Zfp423	MA0116.1	2	*Krt17, Akt1s1*	Zinc-finger
RORA_1	MA0071.1	2	*Krt17, Akt1s1*	Immunity
PPARG::RXRA	MA0065.2	2	*Krt17, Akt1s1*	Vitamin D
Spz1	MA0111.1	2	*Krt17, Akt1s1*	Sex determination
INSM1	MA0155.1	2	*Krt17, Akt1s1*	Zinc-finger
CREB1	MA0018.2	2	*Krt17, Akt1s1*	Neurons
Stat3	MA0144.1	2	*Krt17, Akt1s1*	Erythropoietin
REL	MA0101.1	2	*Krt17, Akt1s1*	NF-κb signaling
EBF1	MA0154.1	2	*Krt17, Akt1s1*	Immunity
SP1	MA0079.2	2	*Krt17, Akt1s1*	Zinc-finger
YY1	MA0095.1	2	*Krt17, Akt1s1*	Immunity
MZF1_5-13	MA0057.1	2	*Krt17, Akt1s1*	Zinc-finger
ELK1	MA0028.1	2	*Krt17, Akt1s1*	ERK signaling
Klf4	MA0039.2	2	*Krt17, Akt1s1*	Cancer
NFATC2	MA0152.1	2	*Krt17, Akt1s1*	Immunity
Arnt::Ahr	MA0006.1	2	*Krt17, Akt1s1*	Inflammation

The expression of *Ak4*, *Ankrd37*, *Mgarp1*, *Slc16a3* and *Tmprss6* was significantly downregulated following FGF23 stimulation for 4 h. The expression of *Mt1*, *Mt2*, *Pdk1* and *Selenbp* tended to be downregulated by FGF23 stimulation for 4 h, but these effects were not significant. Expressions of remaining genes, *Bnip3*, *Cadps2*, *Mt1*, and *Pygl*, were downregulated by FGF23 stimulation for 4 h, as determined using microarray analysis, but not using qPCR. As described above, these differences could be attributable to the use of direct comparisons in the microarray analysis versus the less reliable indirect comparisons by qPCR. Moreover, the expression of *Bnip3*, *Cadps2*, *Mt2*, and *Pygl*, which were not significantly downregulated by FGF23 stimulation for 4 h, was significantly downregulated following stimulation for 2 h. The expression of *Mt1* tended to be downregulated following 2 h FGF23 stimulation. Thus, the downregulation of all genes identified using microarray analysis was confirmed using qPCR for either the 2 h or the 4 h FGF23 stimulation timepoint.

The expression of 10 out of 12 FGF23-downregulated genes was upregulated in response to erythropoietin (Figure 2). According to our bioinformatics analysis, five of the 10 genes, *Bnip3*, *Mt1*, *Mt2*, *Pdk1* and *Slc16a3*, were related to oxidative stress, *Cadps2* was related to neurotransmission, *Pygl* was related to glycogenosis, *Selenbp* was related to cancer and *Tmprss6* was related to androgen signaling. Thus, FGF23 mainly modulated the oxidative stress genes induced by erythropoietin. The effects of erythropoietin on these genes were mediated by STAT1, as shown by the results of an STAT1 knock-down experiment (Figure S2). However, STAT1 phosphorylation was not significantly affected by FGF23 (Figure 3). Expression of the 10 erythropoietin-upregulated genes was suppressed when the cells were stimulated with FGF23 and erythropoietin together (Figure 2). These results indicate that FGF23 modulated the effects of erythropoietin in renal tubule epithelial cells in a STAT1-independent manner and illustrate cross talk between FGF23 and erythropoietin signaling.

Table 4 Transcription factors putatively involved in the downregulation of genes following FGF23 stimulation

Transcription factor	JASPAR ID	No. of target gene hits	Hit genes	Biological function
HOXA5	MA0158.1	12	*Ak4, Ankrd37, Bnip3, Cadps2, Mt1, Pdk1, Pygl, Selenbp1, Slc16a3, Tmprss6, 1700026L06Rik, 2010300C02Rik*	Fat metabolism
Pdx1	MA0132.1	10	*Ak4, Ankrd37, Cadps2, Mt1, Pdk1, Selenbp1, Slc16a3, Tmprss6, 1700026L06Rik, 2010300C02Rik*	Organogenesis
ZEB1	MA0093.1	10	*Ak4, Ankrd37, Bnip3, Cadps2, Pdk1, Pygl, Slc16a3, Tmprss6, 1700026L06Rik, 2010300C02Rik*	Organogenesis
HIF1A ARNT	MA0259.1	9	*Ak4, Ankrd37, Bnip3, Cadps2, Pdk1, Slc16a3, Tmprss6, 1700026L06Rik, 2010300C02Rik*	Oxidative stress
NFATC2	MA0152.1	9	*Ak4, Ankrd37, Cadps2, Pdk1, Pygl, Slc16a3, Tmprss6, 1700026L06Rik, 2010300C02Rik*	Immunity
Nkx2-5	MA0063.1	9	*Ak4, Ankrd37, Bnip3, Cadps2, Pygl, Selenbp1, Tmprss6, 1700026L06Rik, 2010300C02Rik*	Organogenesis
SPIB	MA0081.1	9	*Ak4, Ankrd37, Cadps2, Pdk1, Pygl, Slc16a3, Tmprss6, 1700026L06Rik, 2010300C02Rik*	Organogenesis
USF1	MA0093.1	8	*Ak4, Ankrd37, Bnip3, Cadps2, Pdk1, Slc16a3, 1700026L06Rik, 2010300C02Rik*	Fat metabolism
Arnt	MA0004.1	8	*Ak4, Ankrd37, Bnip3, Cadps2, Pdk1, Slc16a3, 1700026L06Rik, 2010300C02Rik*	Oxidative stress
FOXO3	MA0157.1	7	*Ak4, Cadps2, Pdk1, Pygl, Slc16a3, Tmprss6, 1700026L06Rik*	Organogenesis
Prrx2	MA0075.1	7	*Ankrd37, Cadps2, Pdk1, Selenbp1, Slc16a3, Tmprss6, 2010300C02Rik*	Organogenesis
SRY	MA0084.1	7	*Ankrd37, Cadps2, Pdk1, Pygl, Slc16a3, 1700026L06Rik, 2010300C02Rik*	Sex determination
Sox5	MA0087.1	7	*Ak4, Ankrd37, Cadps2, Pdk1, Selenbp1, 1700026L06Rik, 2010300C02Rik*	Organogenesis
FOXD1	MA0031.1	6	*Ankrd37, Cadps2, Pdk1, Pygl, Tmprss6, 1700026L06Rik*	Oxidative stress
Spz1	MA0111.1	6	*Ak4, Cadps2, Slc16a3, Tmprss6, 1700026L06Rik, 2010300C02Rik*	Sex determination
Nobox	MA0125.1	6	*Ankrd37, Cadps2, Pdk1, Selenbp1, Tmprss6, 2010300C02Rik*	Organogenesis
NFIL3	MA0025.1	4	*Cadps2, Pdk1, Selenbp1, 2010300C02Rik*	Immunity
NFE2L2	MA0150.1	4	*Cadps2, Tmprss6, 1700026L06Rik, 2010300C02Rik*	Oxidative stress
Ddit3 Cebpa	MA0019.1	4	*Bnip3, Cadps2, Pdk1, 1700026L06Rik*	Leukemia
HNF4A	MA0114.1	4	*Cadps2, Pdk1, Pygl, Selenbp1*	Organogenesis
Egr1	MA0162.1	4	*Ak4, Bnip3, Cadps2, Slc16a3*	ERK signaling
HNF1A	MA0046.1	3	*Cadps2, Slc16a3, 2010300C02Rik*	Oxidative stress
STAT1	MA0137.2	3	*Ankrd37, Cadps2, Slc16a3*	Erythropoietin

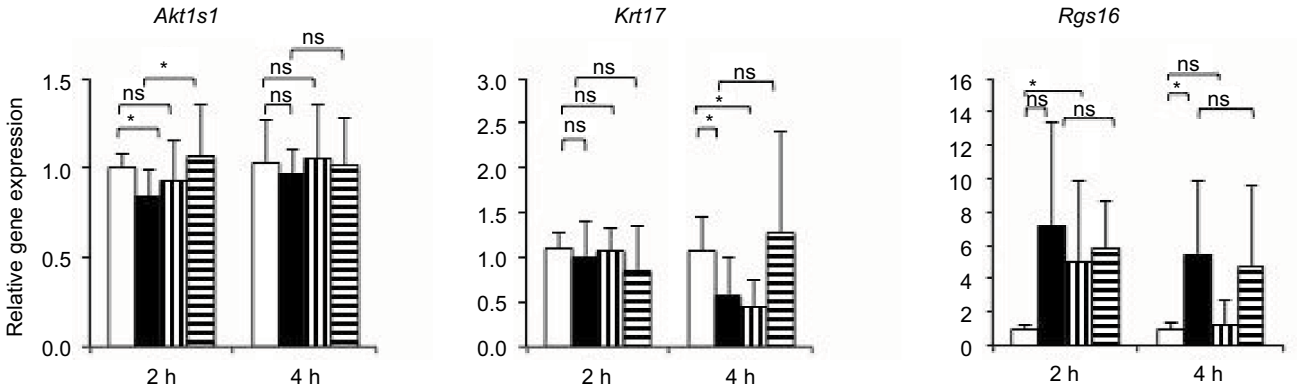

Figure 1 Interactive effects of FGF23 and erythropoietin on the expression of genes upregulated by FGF23.
Notes: mIMCD3 cells were stimulated with erythropoietin with or without FGF23 for 2 or 4 h. Gene expression was measured by quantitative polymerase chain reactions. White bars: no stimulation; black bars: stimulation with 1 U/mL erythropoietin; vertically striped bars: stimulation with 10 ng/mL FGF23; horizontally striped bars: stimulation with 1 U/mL erythropoietin plus 10 ng/mL FGF23. n = 7–10. *$p < 0.05$.
Abbreviation: ns, not significant.

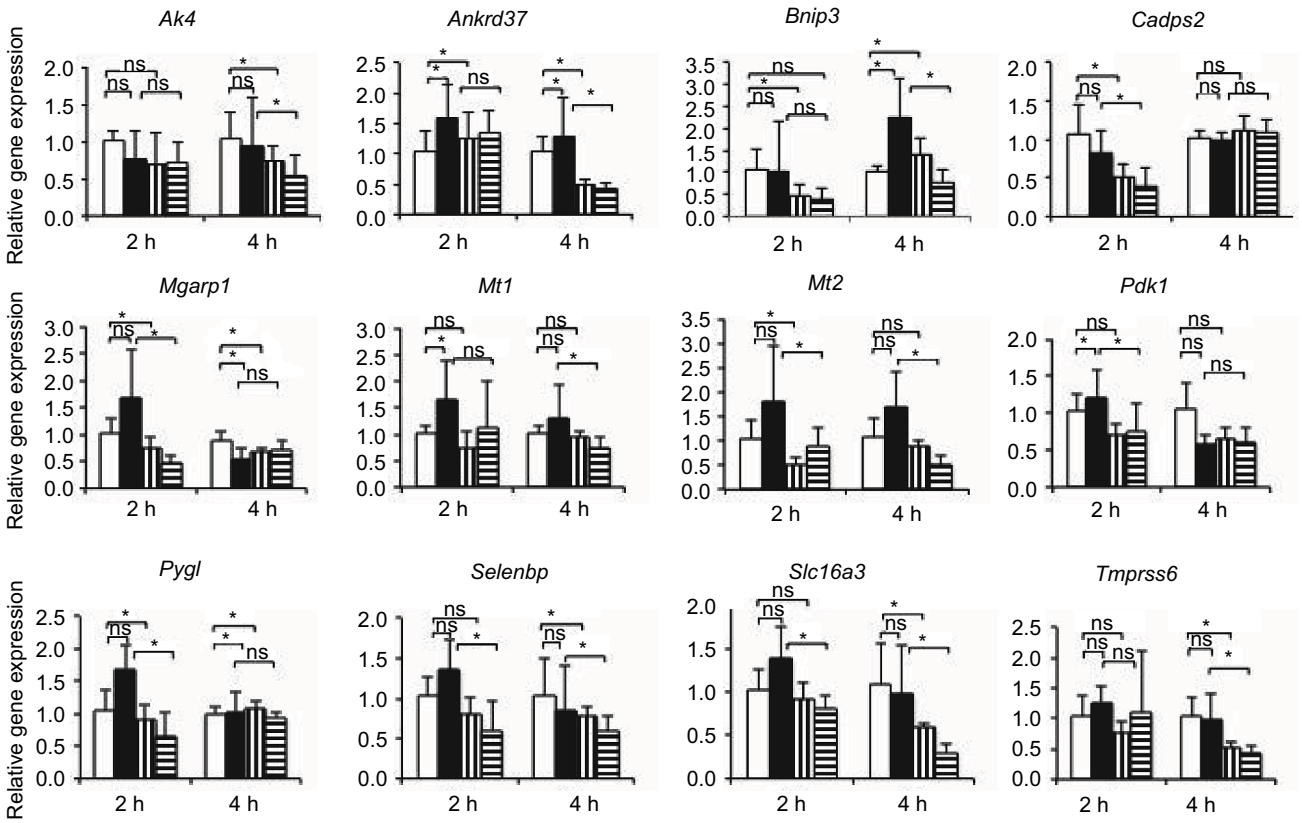

Figure 2 Interactive effects of FGF23 and erythropoietin on the expression of genes downregulated by FGF23.
Notes: mIMCD3 cells were stimulated with erythropoietin with or without FGF23 for 2 or 4 h. Gene expression was measured by quantitative polymerase chain reactions. White bars: no stimulation; black bars: stimulation with 1 U/mL erythropoietin; vertically striped bars: stimulation with 10 ng/mL FGF23; horizontally striped bars: stimulation with 1 U/mL erythropoietin plus 10 ng/mL FGF23. n = 7–10. *$p < 0.05$.
Abbreviation: ns, not significant.

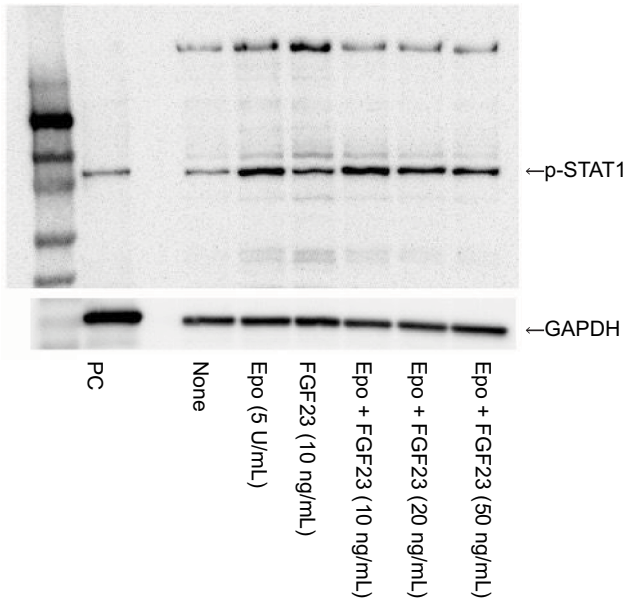

Figure 3 Effect of FGF23 on the phosphorylation of STAT1 induced by erythropoietin.
Notes: mIMCD3 cells were stimulated with the following: 5 U/mL erythropoietin alone; 10 ng/mL FGF23 alone or 5 U/mL erythropoietin plus 10, 20 or 50 ng/mL FGF23. Phosphorylated STAT1 was detected by Western blotting.
Abbreviations: PC, positive control for phosphorylated STAT1 (control cell extract); none, unstimulated cells; Epo, erythropoietin; p-STAT1, phosphorylated STAT1; GAPDH, control for total protein loading.

ERK mediation of the effects of FGF23 on gene expression induced by erythropoietin

ERK is known to mediate the induction of gene expression by FGF23.[15] To investigate whether it also mediates the suppressive effects of FGF23 on the induction of gene by erythropoietin, mIMCD3 cells were costimulated with erythropoietin, FGF23 and an ERK inhibitor. The expression of seven out of 10 erythropoietin-upregulated genes that were suppressed by FGF23, *Ankrd37*, *Mgarp1*, *Mt1*, *Mt2*, *Pygl*, *Slc16a3* and *Selenbp*, was significantly recovered following cotreatment with the ERK inhibitor (Figure 4). Taken together, our results indicate that the mechanism by which FGF23 suppresses the induction of gene expression by erythropoietin might involve inhibitory RNAs that are induced through ERK activation by FGF23.

Discussion

The role of FGF23 has mostly been studied in the field of Ca–P metabolism; however, other biological roles of FGF23 have been reported more recently. Thus, we hypothesized that

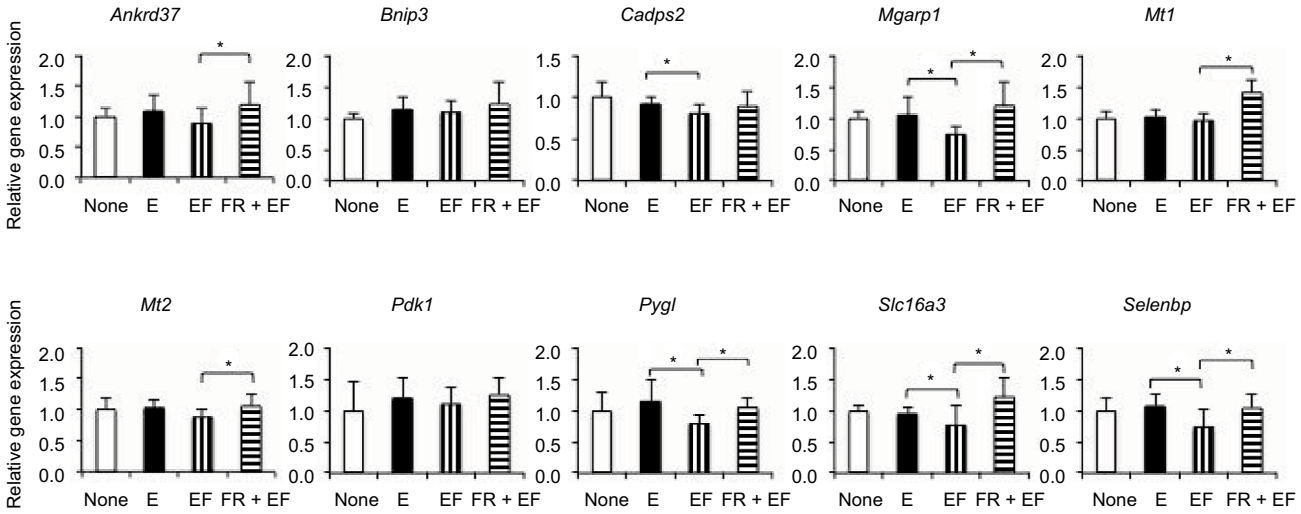

Figure 4 Effects of ERK inhibition on the regulation of gene expression by FGF23 and erythropoietin.
Notes: mIMCD3 cells were treated with erythropoietin alone, with erythropoietin plus FGF23 or with erythropoietin and FGF23 plus the ERK inhibitor, FR180204, for 2 h. Gene expression was measured by quantitative polymerase chain reactions. White bars: no treatment; black bars: 1 U/mL erythropoietin alone (E); vertically striped bars: 1 U/mL erythropoietin plus 10 ng/mL FGF23 (EF); horizontally striped bars: 1 U/mL erythropoietin and 10 ng/mL FGF23 plus 1 μM FR180204 (FR + EF). n = 6. *$p < 0.05$.

FGF23 may have biological roles in renal cells other than Ca–P metabolism. To identify new biological roles of FGF23 in renal tubule epithelial cells, we performed an exhaustive gene expression analysis using DNA microarrays and bioinformatics analysis. As a result, PPARγ and STAT3 were identified as candidate transcription factors for mediating the upregulation of genes by FGF23. Conversely, STAT1 was identified as a candidate for mediating the downregulation of genes by FGF23. STAT1 and STAT3 are also known to mediate the intracellular signaling of erythropoietin. Erythropoietin is known to be involved in the restoration of renal function in patients with renal failure, and its receptor is expressed on renal tubule epithelial cells.[19] Thus, signaling through STAT1 is important in renal epithelial cell function. These observations suggest that FGF23 and erythropoietin might interact to regulate gene expression in renal tubule epithelial cells.

Indeed, we found that the expression of several genes that were downregulated by FGF23 was upregulated by erythropoietin. Furthermore, inhibition of ERK, which mediates FGF23 signaling, reversed the effects of FGF23 on erythropoietin-induced genes. Thus, FGF23 generally suppressed the biological activity of erythropoietin in renal tubule epithelial cells. Only one gene, *Rgs16*, was upregulated by both ligands. Therefore, FGF23 may not exclusively suppress gene expression induced by erythropoietin but also stimulate the expression of some erythropoietin-induced genes.

The physiological roles of erythropoietin in renal tubule epithelial cells have been reported to include the suppression of fibrosis, protection against apoptosis,[23] prevention of renal injury[24] and responses to oxidative stress.[25] These effects can act to prevent the injury of renal tubule epithelial cells. In this study, we showed that FGF23 modulated the expression of genes related to oxidative stress, *Mt1*, *Mt2*, *Ak4*, *Bnip3* and *Pdk1*,[26–30] which were induced by erythropoietin, but not the expression of genes related to other effects of erythropoietin, such as the suppression of fibrosis or apoptosis and the prevention of ischemic injury. Moreover, expression of the oxidative stress gene, *Nrf2*,[31] which has been reported to have protective effects against renal tubule cell injury, was not suppressed by FGF23. Furthermore, not all genes related to oxidative stress have a protective effect against renal tubule epithelial cell injury, because *Nupr1*, another gene related to oxidative stress, can act to potentiate the injury of renal tubule epithelial cells.[32] In light of these considerations, FGF23 may cooperate with erythropoietin to protect renal tubule epithelial cells against injury by suppressing the expression of oxidative stress genes that would have harmful effects if induced by erythropoietin alone. We aim to test this hypothesis in a future study.

We also found that erythroblasts expressed both EpoR and Klotho (Figure 5). This observation similarly may be attributable to the interaction of erythropoietin and FGF23 in these cells. It may cause the erythropoietin-resistant anemia seen in patients with renal failure, whose serum levels of FGF23 are extremely high.[33]

According to our Western blot analysis, FGF23 did not influence the STAT1 phosphorylation that was induced

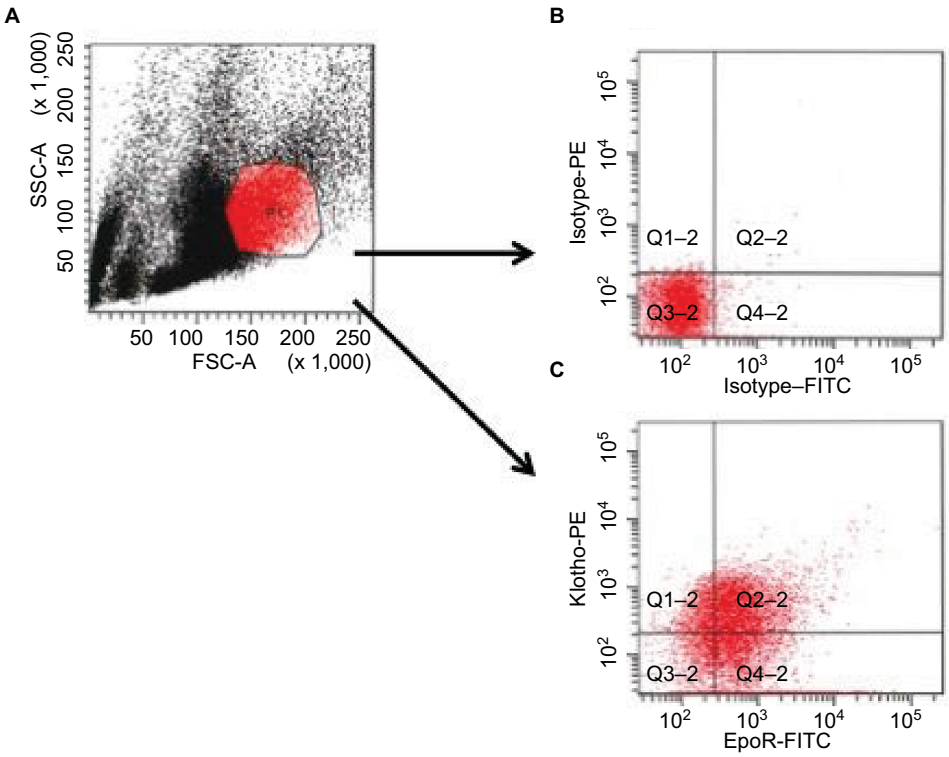

Figure 5 Expression of EpoR and Klotho protein by mouse bone marrow cells.
Notes: To confirm that mouse bone marrow cells expressed EpoR and Klotho, these cells were assayed by flow cytometry. Aliquots of 10^6 bone marrow cells were incubated with anti-EpoR–FITC and anti-Klotho–PE antibodies, and the cells were analyzed on an FACS Aria flow cytometer (BD Biosciences, San Jose, CA, USA). (**A**) Erythroblast gating (P1) of bone marrow cells (FSC-A, SSC-A). (**B**) P1 gated, isotype controls. (**C**) P1 gated, EpoR- and Klotho-labeled. Bone marrow cells were obtained from the femurs and tibias of male C57BL/6J mice. PE was conjugated to an anti-human Klotho monoclonal antibody (cat. no. KO603) using a Phycoerythrin Labeling Kit-NH2 (Dojindo Molecular Technologies, Kumamoto, Japan). FITC was conjugated to an anti-mouse EpoR monoclonal antibody (cat. no. ab56310) using a Fluorescein Labeling Kit-NH2 (Dojindo Molecular Technologies).
Abbreviations: FITC, fluorescein isothiocyanate; PE, phycoerythrin; FSC-A, forward scatter; SSC-A, side scatter.

by erythropoietin. Thus, FGF23 would not directly affect STAT1 activity. A possible alternative mechanism of FGF23–erythropoietin cross talk involves both signaling pathways acting directly on the promoters of target genes. Recently, there have been reports that nonprotein-coding genes can act as regulatory elements to suppress the expression of protein-coding genes.[34,35] In this study, the expression of five nonprotein-coding genes was upregulated by FGF23. Thus, the mechanism of cross talk between FGF23 and erythropoietin might involve these regulatory nonprotein-coding genes. We have not yet clarified which nonprotein-coding genes are involved, but we would like to address this in a future study.

There were some limitations to this study. One is that by changing the criteria for identification of upregulated or downregulated genes, other meaningful genes might be discovered. Another is that the available bioinformatics data are increasing all the time, but we were only able to use the bioinformation accumulated to date. Hence, additional transcription factors may be identifiable in similar studies conducted in the future. Furthermore, the transcription factors identified in this study other than PPARγ, STAT1 and STAT3 may have important biological roles in renal epithelial cells, which should be clarified in future studies. The last is that we examined only one renal tubule epithelial cell line. Thus, different results may be obtained using cell lines other than mIMCD3.

Conclusion

In summary, we attempted to identify new biological roles of FGF23 in renal tubule epithelial cells. Our results raise the possibility of cross talk between FGF23 and erythropoietin signaling. Because FGF23 and erythropoietin play important roles in the pathology of patients with chronic renal failure, elucidation of such cross talk could contribute to a better understanding of this pathological condition.

Abbreviations

Ca-P, calcium–phosphorus
PVDF, polyvinylidene difluoride
qPCR, quantitative polymerase chain reaction

SD, standard deviation

TBST, Tris-buffered saline (50 mM Tris, 150 mM NaCl, pH 7.6) with 0.05% Tween 20

Acknowledgments

This work was supported by a Grant in Aid for Scientific Research (KAKENHI) (grant number 16K09651) and Wakayama Kidney Foundation. The authors thank Ms. M Matsudaira and Ms. Y Doi for providing excellent secretarial support. They also thank Edanz Group (www.edanzediting.com/ac) for editing a draft of this manuscript.

Disclosure

The authors report no conflicts of interest in this work.

References

1. Martin A, David V, Quarles LD. Regulation and function of the FGF23/klotho endocrine pathways. *Physiol Rev*. 2012;92:131–155.
2. Shimada T, Kakitani M, Yamazaki Y, et al. Targeted ablation of Fgf23 demonstrates an essential physiological role of FGF23 in phosphate and vitamin D metabolism. *J Clin Invest*. 2004;113:561–568.
3. Razzaque MS, Sitara D, Taguchi T, et al. Premature aging-like phenotype in fibroblast growth factor 23 null mice is a vitamin D-mediated process. *FASEB J*. 2006;20:720–722.
4. Tsujikawa H, Kurotaki Y, Fujimori T, et al. Klotho, a gene related to a syndrome resembling human premature aging, functions in a negative regulatory circuit of vitamin D endocrine system. *Mol Endocrinol*. 2003;17:2393–2403.
5. Graciolli FG, Neves KR, Barreto F, et al. The complexity of chronic kidney disease-mineral and bone disorder across stages of chronic kidney disease. *Kidney Int*. 2017;91:1436–1446.
6. Gutierrez OM. Fibroblast growth factor 23 and heart failure: the plot thickens. *Nephrol Dial Transplant*. 2016;31:688–690.
7. Raimann A, Ertl DA, Helmreich M, et al. Fibroblast growth factor 23 and Klotho are present in the growth plate. *Connect Tissue Res*. 2013;54:108–117.
8. Masuda Y, Ohta H, Morita Y, et al. Expression of Fgf23 in activated dendritic cells and macrophages in response to immunological stimuli in mice. *Biol Pharm Bull*. 2015;38:687–693.
9. Okada S, Yoshida T, Hong Z, et al. Impairment of B lymphopoiesis in precocious aging (klotho) mice. *Int Immunol*. 2000;12:861–871.
10. Saji F, Shiizaki K, Shimada S, et al. Regulation of fibroblast growth factor 23 production in bone in uremic rats. *Nephron Physiol*. 2009;111:59–66.
11. Nakashima Y, Mima T, Yashiro M, et al. Expression and localization of fibroblast growth factor (FGF)23 and Klotho in the spleen: its physiological and functional implications. *Growth Factors*. 2016;34:196–202.
12. Mitobe M, Yoshida T, Sugiura H, et al. Oxidative stress decreases klotho expression in a mouse kidney cell line. *Nephron Exp Nephrol*. 2005;101(2):e67–e74.
13. Bennett L, Palucka AK, Arce E, et al. Interferon and granulopoiesis signatures in systemic lupus erythematosus blood. *J Exp Med*. 2003;197:711–723.
14. Ishikawa S, Mima T, Aoki C, et al. Abnormal expression of the genes involved in cytokine networks and mitochondrial function in systemic juvenile idiopathic arthritis identified by DNA microarray analysis. *Ann Rheum Dis*. 2009;68:264–272.
15. Urakawa I, Yamazaki Y, Shimada T, et al. Klotho converts canonical FGF receptor into a specific receptor for FGF23. *Nature*. 2006;444(7120):770–774.
16. Ogilvie M, Yu X, Nicolas-Metral V, et al. Erythropoietin stimulates proliferation and interferes with differentiation of myoblasts. *J Biol Chem*. 2000;275(50):39754–39761.
17. Miyake K, Utsugisawa T, Flygare J, et al. Ribosomal protein S19 deficiency leads to reduced proliferation and increased apoptosis but does not affect terminal erythroid differentiation in a cell line model of Diamond-Blackfan anemia. *Stem Cells*. 2008;26(2):323–329.
18. Ohori M, Kinoshita T, Okubo M, et al. Identification of a selective ERK inhibitor and structural determination of the inhibitor-ERK2 complex. *Biochem Biophys Res Commun*. 2005;336(1):357–363.
19. Kapil A, Singh JP, Kaur T, et al. Involvement of peroxisome proliferator-activated receptor gamma in vitamin D-mediated protection against acute kidney injury in rats. *J Surg Res*. 2013;185:774–783.
20. Haq R, Halupa A, Beattie BK, et al. Regulation of erythropoietin-induced STAT serine phosphorylation by distinct mitogen-activated protein kinases. *J Biol Chem*. 2002;277:17359–17366.
21. Furumatsu Y, Nagasawa Y, Hamano T, et al. Integrated therapies including erythropoietin decrease the incidence of dialysis: lessons from mapping the incidence of end-stage renal disease in Japan. *Nephrol Dial Transplant*. 2008;23:984–990.
22. Peixoto BR, Vêncio RZ, Egidio CM, et al. Evolution of reference-based two-color methods for measurement of gene expression rations spotted cDNA microarrays. *BMC Genomics*. 2006;7:35.
23. Brines M. The therapeutic potential of erythropoiesis-stimulating agents for tissue protection: a tale of two receptors. *Blood Purif*. 2010;29(2):86–92.
24. Imamura R, Moriyama T, Isaka Y, et al. Erythropoietin protects the kidneys against ischemia reperfusion injury by activating hypoxia inducible factor-1alpha. *Transplantation*. 2007;83(10):1371–1379.
25. Yamazaki S, Souma T, Hirano I, Pan X, Minegishi N, Suzuki N, Yamamoto M. A mouse model of adult-onset anaemia due to erythropoietin deficiency. *Nat Commun*. 2013;4:1950.
26. Di Foggia V, Zhang X, Licastro D, et al. Bmi1 enhances skeletal muscle regeneration through MT1-mediated oxidative stress protection in a mouse model of dystrophinopathy. *J Exp Med*. 2014;211:2617–2633.
27. Ling XB, Wei HW, Wang J, et al. Mammalian metallothionein-2A and oxidative stress. *Int J Mol Sci*. 2016;6:17.
28. Awan MU, Hasan M, Iqbal J, et al. Neuroprotective role of BNIP3 under oxidative stress through autophagy in neuroblastoma cells. *Mol Biol Rep*. 2014;41:5729–5734.
29. Kume S, Uzu T, Horiike K, et al. Calorie restriction enhances cell adaptation to hypoxia through Sirt1-dependent mitochondrial autophagy in mouse aged kidney. *J Clin Invest*. 2010;120(4):1043–1055.
30. Anthony RG, Khan S, Costa J, et al. The Arabidopsis protein kinase PTI1-2 is activated by convergent phosphatidic acid and oxidative stress signaling pathways downstream of PDK1 and OXI1. *J Biol Chem*. 2006;281:37536–37546.
31. Wu QQ, Wang Y, Senitko M, et al. Bardoxolone methyl (BARD) ameliorates ischemic AKI and increases expression of protective genes Nrf2, PPARγ, and HO-1. *Am J Physiol Renal Physiol*. 2011;300(5):F1180–F1192.
32. Amrouche L, Desbuissons G, Rabant M, et al. MicroRNA-146a in human and experimental ischemic AKI: CXCL8-dependent mechanism of action. *J Am Soc Nephrol*. 2017;28:479–493.
33. Mehta R, Cai X, Hodakowski A, et al. Fibroblast growth factor 23 and anemia in the Chronic Renal Insufficiency Cohort Study. *Clin J Am Soc Nephrol*. 2017;12(11):1795–1803.
34. Galichon P, Bataille A, Vandermeersch S, et al. Stress response gene Nupr1 alleviates cyclosporin A nephrotoxicity in vivo. *J Am Soc Nephrol*. 2017;28:545–556.
35. Selbach M, Schwanhäusser B, Thierfelder N, et al. Widespread changes in protein synthesis induced by microRNAs. *Nature*. 2008;455:58–63.

Supplementary materials

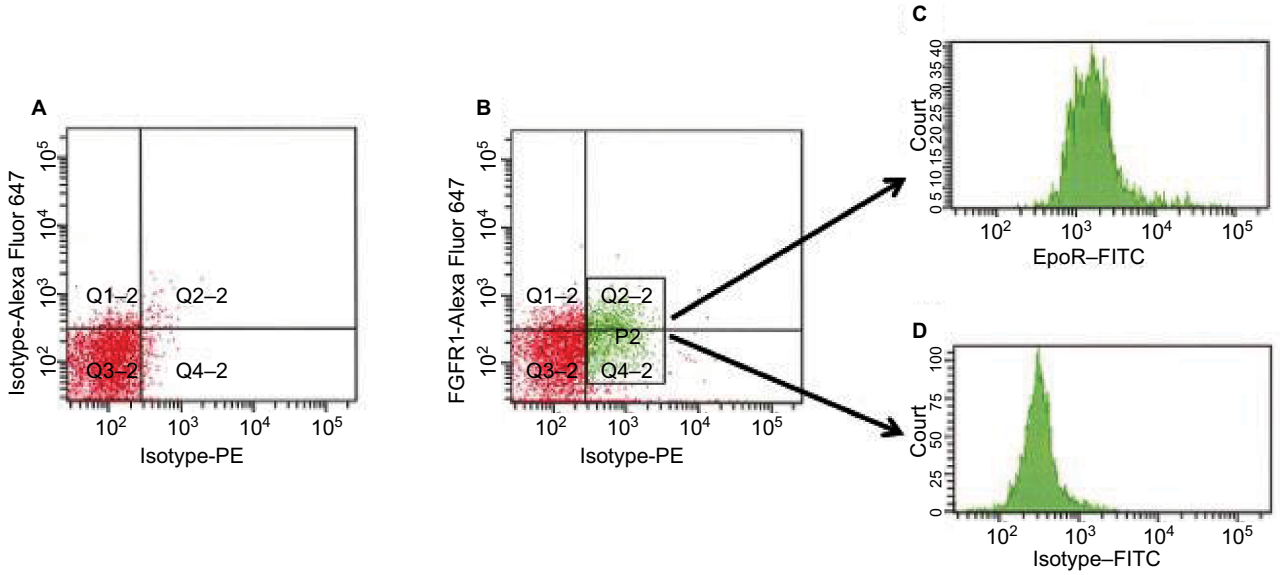

Figure S1 The mouse renal epithelial cell line, mIMCD3, expressing Klotho, FGFR1 and EpoR protein.

Notes: To confirm that mouse renal epithelial cell line, mIMCD3, expressed Klotho, FGFR1 and EpoR, the cells were assayed by flow cytometry. Aliquots of 10^6 mIMCD3 cells were incubated with anti-Klotho/PE and anti-FGFR1/Alexa Fluor 647 antibodies, and anti-EpoR/FITC antibodies, and the cells were analyzed on an FACS Aria flow cytometer (BD Biosciences, San Jose, CA, USA): (**A**) isotype controls. (**B**) Klotho$^+$ FGFRI$^+$ gated. (**C**) Klotho$^+$ FGFRI$^+$ gated, EpoR. (**D**) Klotho$^+$ FGFRI$^+$ gated, isotype controls. PE was conjugated to anti-human Klotho monoclonal antibodies (cat. no. KO603) using a Phycoerythrin Labeling Kit-NH2 (Dojindo Molecular Technologies, Kumamoto, Japan). Alexa Fluor 647 was conjugated to anti-FGFR1 (cat. no. M19B2) using an Alexa Fluor 647 Microscale Protein Labeling Kit (Thermo Fisher Scientific, Waltham, MA, USA). FITC was conjugated to anti-mouse EpoR monoclonal antibodies (cat. no. ab56310) using a Fluorescein Labeling Kit-NH2 (Dojindo Molecular Technologies).

Abbreviations: FITC, fluorescein isothiocyanate; PE, phycoerythrin.

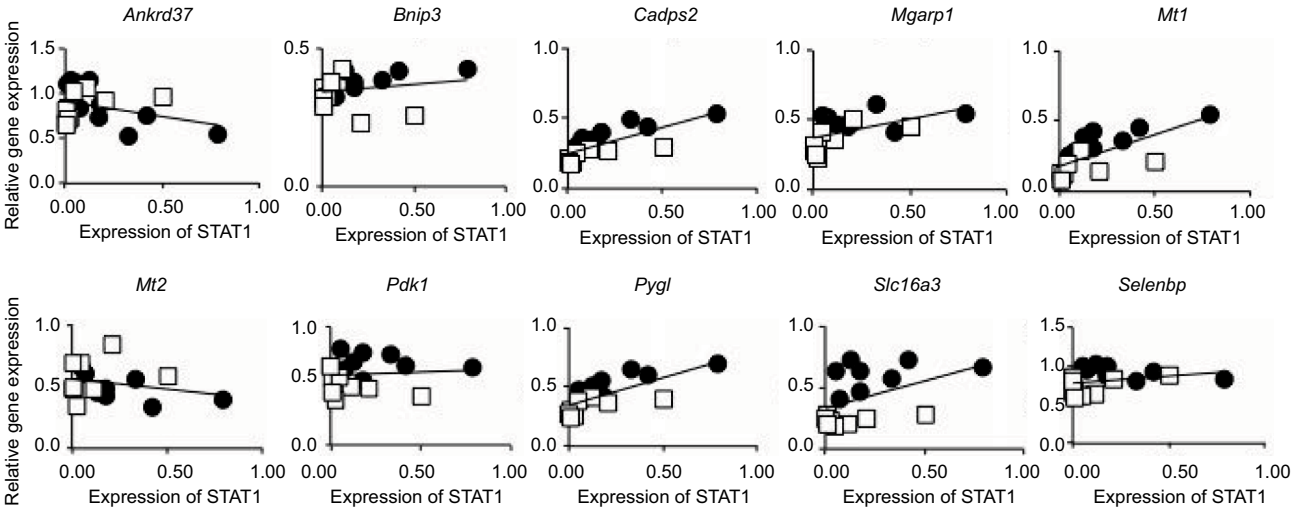

Figure S2 Effects of STAT1 knockdown on the upregulation of genes by erythropoietin.

Notes: A knockdown construct for STAT1 was purchased from GeneCopoeia (Rockville, MD, USA). The STAT1 knockdown sequence was inserted into the pcDNA3.1 vector (Thermo Fisher Scientific, Waltham, MA, USA). pcDNA3.1, either with or without the STAT1 knockdown sequence, was transferred into mIMCD3 cells. These cells were then stimulated with 1 U/mL erythropoietin, for either 2 or 4 h. RNA was extracted, and gene expression was analyzed using quantitative polymerase chain reactions, as described in the "Materials and methods" section. The expression of *Bnip3*, *Cadps2*, *Mgarpl*, *Mtl*, *Pygl* and Selenbp was correlated with that of STAT1, suggesting that the induction of these genes was mediated by STAT1. For each gene, the line-of-best-fit showing the correlation with STAT1 expression is shown. Black circles: cells treated with pcDNA3.1 without the STAT1 knockdown sequence; white squares: cells treated with pcDNA3.1 with the STAT1 knockdown sequence.